ARTICLE

Quantitative Analysis of the GAL4/UAS System in *Drosophila* Oogenesis

Lea A. Goentoro,[1,2] Nir Yakoby,[1,2] Joseph Goodhouse,[3] Trudi Schüpbach,[3] and Stanislav Y. Shvartsman[1,2]*

[1]Department of Chemical Engineering, Princeton University, Princeton, New Jersey
[2]Lewis-Sigler Institute for Integrative Genomics, Princeton University, Princeton, New Jersey
[3]Department of Molecular Biology, Princeton University, Princeton, New Jersey

Received 26 July 2005; Accepted 19 November 2005

Summary: The GAL4/UAS system is extensively used for targeted gene expression in *Drosophila*, but the strength of the GAL4 drivers and their effects on target genes are rarely quantified. Quantitative information about the strength of the perturbations introduced by the GAL4/UAS system would further expand the usefulness of the GAL4/UAS system in studying gene functions and developmental processes. We have developed an assay to determine the relative level of expression for target genes tagged with green fluorescent protein (GFP). Our assay enables the relative quantitation of fluorescent proteins within specific cell types and developmental time windows in living eggs/embryos, and permits the analysis of samples from a broad expression range. We illustrate the assay using a panel of four GAL4 drivers and three UAS responder lines in *Drosophila* oogenesis, discuss the issues associated with the interpretation of the quantitative data, and correlate our results with the analysis of the GAL4/UAS system at the transcript level. The imaging-based strategy described here can be used to quantify other GAL4 drivers in *Drosophila* and other organisms. genesis 44:66–74, 2006. Published 2006 Wiley-Liss, Inc.†

Key words: quantitative fluorescence; *Drosophila*; GAL4/UAS; GFP; EGFP; EGFR

INTRODUCTION

The use of the GAL4/UAS system for targeted gene expression was first introduced in *Drosophila* by Brand and Perrimon (1993). Random genomic insertions of the yeast transcriptional activator GAL4 allow expression of target genes fused to the UAS^{GAL4} sequences. Large numbers of such GAL4 insertions have been isolated by many laboratories and are widely used to ectopically express genes of interest (see Duffy, 2001, for review of the GAL4/UAS system in *Drosophila*). The GAL4/UAS system is also used in mice and has recently been introduced into *Xenopus* and zebrafish (Ornitz *et al.*, 1991; Hartley *et al.*, 2001; Scheer and Campos-Ortega, 1999). The high degree of spatiotemporal specificity offered by the GAL4/UAS system makes it a useful tool for studying developmental processes. Correlating the level of perturbations with the induced responses, at the level of gene expression or tissue architecture, can yield quantitative insights into processes such as cell fate induction by extracellular signals. The strength of perturbations introduced through the GAL4/UAS system has been characterized mostly qualitatively, through the phenotypic effects. Since the induced phenotypes may not correlate with the strength of perturbations in a straightforward manner, an independent quantitation of perturbations induced by the GAL4/UAS systems is necessary. We report here a quantitative assay to directly estimate the relative strength of perturbations introduced through the GAL4/UAS system in living tissues.

The assay we developed involves UAS responder lines in which the target genes were tagged with the enhanced green fluorescent protein (EGFP). The use of GFP as a molecular tag has increasingly become the choice strategy to visualize, track, and quantify proteins of interests (see review by Lippincott-Schwartz and Patterson, 2003). Our goal is to estimate the relative amount of fluorescent proteins from the relative fluorescence intensities using confocal microscopy. Correlating changes in fluorescence intensities to relative quantities of tagged proteins requires that all imaging settings (e.g., illumination power, scanning parameters, lightpath and detector settings) be kept constant for all samples (Pawley, 2000; Piston *et al.*, 1999). In practice, this requirement is greatly limiting, mainly for three reasons. First, there is a large number of variables to be kept constant (Pawley, 2000). Second, even if all variables can be kept constant, a given imaging setting may not be optimal for all samples, especially for samples with very different fluorescence intensities. Third,

†This article includes Supplementary Material available via the Internet at http://www.interscience.wiley.com/jpages/1526-954X/suppmat.

*Correspondence to: S.Y. Shvartsman, Carl Icahn Laboratory, Lewis-Sigler Institute for Integrative Genomics, Princeton University, Princeton, NJ 08544.
E-mail: stas@princeton.edu

Published online 00 Month 2006 in
Wiley InterScience (www.interscience.wiley.com).
DOI: 10.1002/gene.20184

large samples, such as eggs or embryos, have to be imaged separately and multiple imaging sessions are required to collect a statistically significant number of data points. In this case, instrument fluctuations and differences in sample preparation will introduce systematic error in the data.

Because of these difficulties, relative quantitation of fluorescence intensities is mostly performed with the samples imaged together on one slide or within a short time frame (e.g., less than 30 min) to avoid any significant drift in the instrument. Alternatively, protocols for obtaining the absolute number of molecules from the corresponding fluorescence intensities have been developed (Hirschberg *et al.*, 1998; Piston *et al.*, 1998). These protocols rely on imaging the sample in parallel with a reference standard slide, made of mounted dye solutions with known concentrations. Both strategies can quickly become cumbersome for large samples for which multiple separate captures are required for collecting statistically meaningful data. A ratiometric method for imaging *Xenopus* embryos was recently developed in which a reference dye is injected into the embryo and used to correct the three-dimensional effects imaged at the same time as the fluorescent protein of interest (Dmochowski *et al.*, 2002). Using an internal reference dye is an attractive way of tracking fluctuations in systems where injection can be easily done, but again may become time-consuming for analyzing a large number of samples.

In this study, we utilized the AOTF (acousto-optic tunable filter) in the laser-scanning confocal microscopy (LSCM) as both an internal reference and a tunable parameter, circumventing the need for reference slide and additional dyes. As an internal reference, we combined the AOTF setting with the laser power measurement as a means to track instrument fluctuations. Adjusting the AOTF to maximize the dynamic range of the fluorescence emission, thus avoiding oversaturating or undersampling the samples, is a common practice in automated data collection. We used the imaging protocol to analyze the GAL4/UAS system in *Drosophila* oogenesis. Our measurements allowed us to rank the strength of four frequently used GAL4 drivers, which we confirmed in parallel analysis using quantitative reverse transcriptase polymerase chain reaction (RT-PCR). We demonstrate that our strategy yields statistically reproducible results, which enable us to distinguish as little as a 1.5-fold difference in the fluorescence intensities.

RESULTS AND DISCUSSION

Spatial Profiles of the GAL4-Induced Gene Expression

The four GAL4 drivers used in this study, 55B, T155, GR1, and CY2, express GAL4 protein in the follicular epithelium of the developing *Drosophila* egg (see Spradling, 1993, for review of *Drosophila* oogenesis). The drivers had been previously ranked based on the induced lacZ expression and the eggshell phenotypes generated by crossing these drivers to the constitutively active form of the epidermal growth factor receptor (EGFR; Queenan, 1997). These GAL4 lines were crossed to three UAS lines to drive the expression of EGFP by itself (UAS-EGFP; Halfon *et al.,* 2002), an EGFP-tagged *Drosophila* EGFR (UAS-EGFR-EGFP; a gift from J. Duffy), and an EGFP-tagged Kekkon1 (UAS-Kekkon1-EGFP), a transmembrane protein and inducible inhibitor of *Drosophila* EGFR signaling (Alvarado *et al.,* 2004).

The spatial profiles of the four GAL4 drivers in the early stage 10A egg chambers are shown in Figure 1 (staging of oogenesis is based on Spradling, 1993). EGFP appears to be uniform, while EGFR-EGFP and Kekkon1-EGFP are both expressed in a punctate pattern. Fluorescent signal is observed within an anterior band of 5–10 cell rows in 55B, and uniformly throughout the follicular epithelium in the other three drivers. In all four drivers the GAL4-induced expression is highly variegated in space; the variegation appears to be random in space and remains constant for at least 30 min (data not shown).

Quantitative Fluorescence Assay

Keeping all imaging settings constant is difficult for examining samples with more than 5-fold difference in their expression levels (as is the case for our panel of GAL4 drivers). In this case, an imaging setting that optimizes the "weak" sample would saturate the "strong" sample. In addition, day-to-day instrument fluctuations can introduce systematic error in measurements from different imaging sessions. Our imaging strategy addresses both problems (Fig. 2; see Supplementary Material for the full description of the assay and the calibration procedures). Our approach relies on the linear dependence of the observed fluorescence intensity on the laser power. This linear correlation is optimized in our experiments in the following ways. First, the choice of EGFP minimizes photobleaching and allows us to work in a low laser-power range where fluorescence saturation is minimal (see Lippincott-Schwartz and Patterson, 2003; Sandison et al., 1995, for review). Second, to avoid pixel saturation and maximize signal-to-noise ratio, we adjusted the AOTF setting in imaging each egg chamber. The AOTF, which ranges from 0–100%, controls the amount of laser intensity that arrives at the sample. Since the laser intensity arriving at the sample is a linear function of the AOTF setting (see Supplementary Material), data taken at different AOTF settings can be normalized to the same arbitrarily chosen reference AOTF value (we used AOTF = 1), where quantitation can then be performed. In short, we use the AOTF as a tunable parameter in our imaging setting, which allows us to quantify samples from a broad expression range. Finally, we keep track of the instrument fluctuations by calibrating the laser power in each imaging session (see Supplementary Material).

With the assay described, we can now compare data taken from different experiments, thus eliminating the need to analyze all samples within the same imaging session. The fluorescence ratios obtained with our assay are

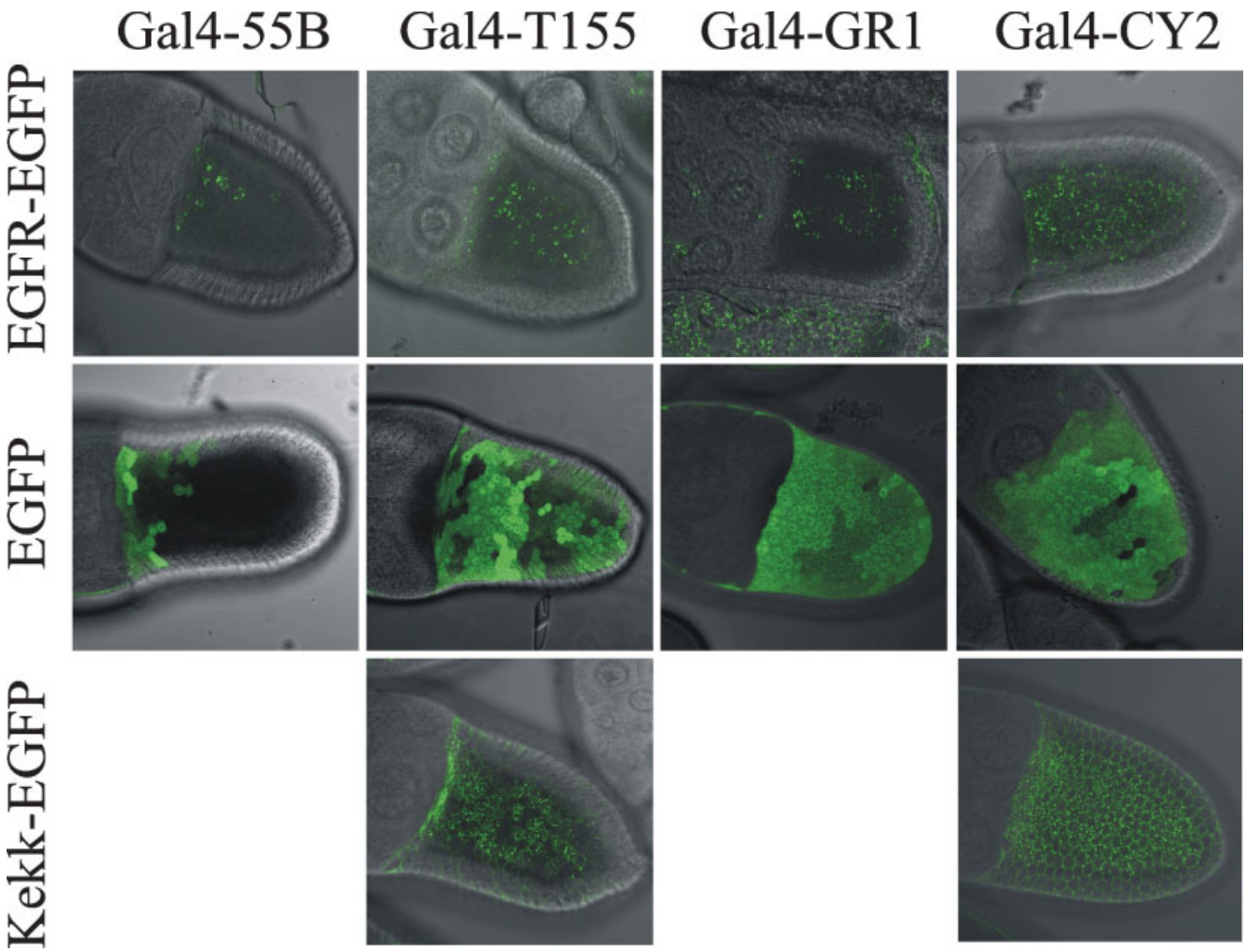

FIG. 1. The pattern of GAL4/UAS expression in early stage 10A egg chambers. Rows 1–3: UAS-EGFR-EGFP, UAS-EGFP, UAS-Kekkon-EGFP. Columns 1–4: GAL4-55B, GAL4-T155, GAL4-GR1, and GAL4-CY2.

reproducible with a coefficient of variation (CV) of 10% (see Supplementary Material). We also validated our assay in vitro with dye solutions of known concentrations (see Supplementary Material).

Relative Strength of the GAL4 Drivers Based on the Fluorescence Assay

Focusing on a particular stage of egg development (early stage 10A, which spans <6 h), we first determined the variability of fluorescence intensity in individual egg chambers (Fig. 3). We calculated the CV of every GAL4/UAS pair and found that the average CV within the selected time window was 26% (Table 1). These measurements enable a rough estimate of the degree to which each particular image is representative of the population of samples generated by a particular GAL4/UAS pair.

The measured fluorescence ratios from the three UAS responder lines are shown in Figure 4 and Table 2. Significantly, we find that the measured fluorescence ratios depend on the nature of the UAS responder (Fig. 4). For example, the GR1/55B and CY2/55B ratios measured using UAS-EGFP are higher than those measured using UAS-EGFR-EGFP (Fig. 4A). The differences seen across the responder lines arise from the differences in the stability of the responder proteins (or transcripts). The measured fluorescence ratios reflect not only the relative strength of GAL4 activation in the drivers, but also the relative accumulation of the responder proteins (or transcripts) prior to the stage where the measurement is made. Thus, the fluorescence ratios reported in Table 2 represent the relative amount of total fluorescent proteins present in the cells at the time of the measurement.

The extent to which prior accumulation contributes to the measured fluorescence ratio depends on the stability of the responder protein/transcript. The more stable the responder protein/transcript, the more the measured fluorescence ratio will be distorted by prior accumulation. This is the case for measurements made in UAS-EGFP. The less stable the responder protein/tran-

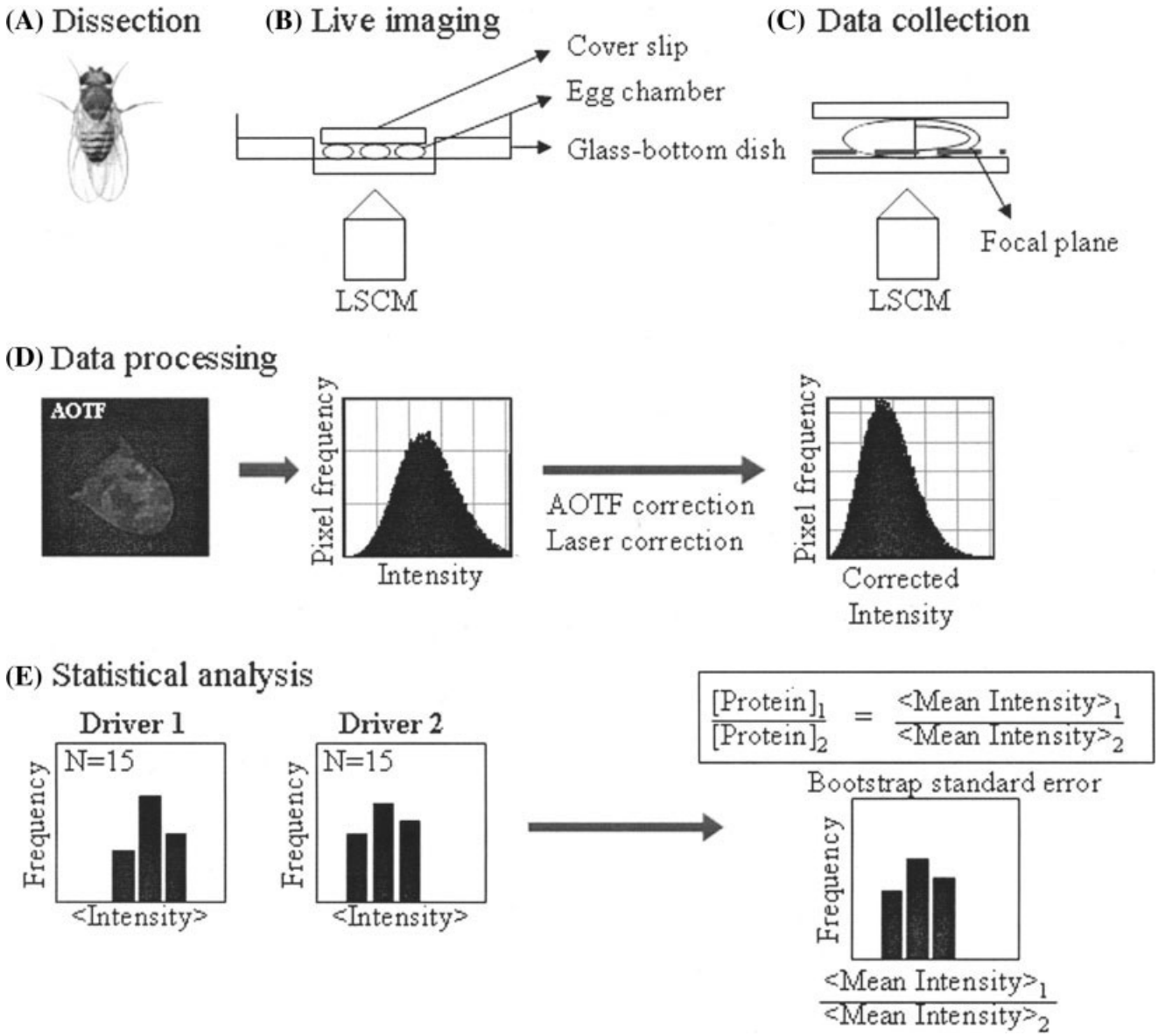

FIG. 2. Overview of the fluorescence assay. **a,b:** Egg chambers were dissected from female flies right before the imaging experiment and mounted on a dish, immersed in fly growth medium. **c:** Imaging in a laser-scanning confocal microscope (LSCM) is optimized for each sample by adjusting the acousto-optic tunable filter (AOTF); instrument fluctuations were tracked by calibrating the laser output. **d:** The fluorescence data is corrected for AOTF and laser fluctuations. **e:** A histogram of mean intensities is built from ~30 images. The protein ratio is computed from the ratio between two corresponding histograms of mean intensities. Bootstrap statistics are used to compute the standard error of the protein ratio (Efron and Tibshirani, 1994). [Color figure can be viewed in the online issue, which is available at www.interscience.wiley.com.]

script, the more closely the measured fluorescence ratios will represent the relative transcriptional strength of the GAL4 drivers. This is the case for UAS-EGFR-EGFP and UAS-Kekkon-EGFP. Finally, the stronger the drivers, the stronger the effects of prior accumulation on the measured fluorescence ratios will be. For weak drivers, such as 55B and T155, prior accumulation appears to be negligible and the same fluorescence ratio is obtained in UAS-EGFP and UAS-EGFR-EGFP (Fig. 4A). Based on our results, we caution against the use of stable free EGFP for quantitative purposes, and recommend whenever possible the use of the EGFP-tagged version of the protein of interest.

Comparison Between Fold Change in the Fluorescence and Transcript Level

We compared the fluorescence-based driver strengths with those obtained with quantitative real-time PCR (qRT-PCR; with primers for EGFP). The qRT-PCR-based

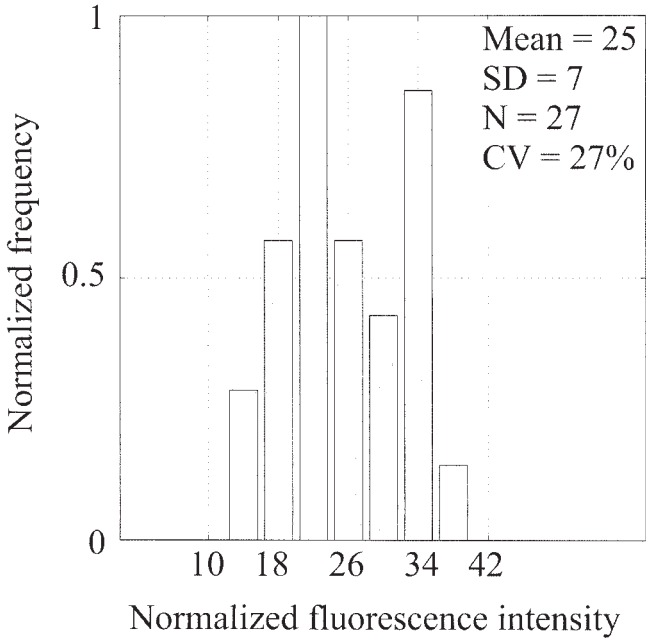

FIG. 3. Variability of GAL4 expression. A histogram of fluorescence intensity for GAL4-CY2/UAS-EGFR-EGFP egg chambers.

assay yields the relative amount of the transcripts in stage 9–10 egg chambers in oogenesis. Since the time window of the qRT-PCR assay is wider than that in the fluorescence assay, a direct quantitative comparison between the results from the two assays was not possible and we were mainly interested in comparing the rank of the drivers obtained with the two techniques. With a single exception (GR1 and T155 driving EGFP), the rank of the drivers was found to be the same in the fluorescence and qRT-PCR assays. Interestingly, the relative amount of the proteins determined by the fluorescence assay was not very different from the relative amount of the transcripts determined by qRT-PCR (Fig. 5).

GAL4-Induced Overexpression Correlates With the Changes in the Target Genes

Finally, we observed that the relative strength of the drivers determined by the fluorescence assay correlated with the corresponding biological effects. As an example, we followed the transcriptional response to expression of EGFR-EGFP using three spatially uniform drivers (T155, GR1, and CY2). Misexpression of EGFR-EGFP in the follicle cells leads to dorsalized eggshells and/or ectopic dorsal appendage material (results not shown), indicative of increased EGFR signaling. We used qRT-PCR to follow the changes in the transcript level of EGFR-EGFP and two of its transcriptional targets in the follicle cells: *kekkon*, which is induced by EGFR signaling, and *pipe*, which is repressed by EGFR signaling (Ghiglione *et al.*, 1999; Sen *et al.*, 1998). We found that the transcript levels of *kekkon* and *pipe* correlated with the increase in the level of EGFR-EGFP transcript and with the rank of the drivers obtained through the fluorescence measurement (Fig. 6). While ranking of the GAL4 drivers by their biological effects provides a consistent qualitative measure of their strength, only the fluorescence-based measurement of the reporter expression allows a direct quantitative comparison of protein levels at any given stage and in any cell type of interest.

Table 1
Variability of GAL4 Expression

	EGFR-EGFP		EGFP		Kekkon-EGFP	
	N	CV (%)	N	CV (%)	N	CV (%)
GAL4-55B	13	20.4	19	57.3	—	—
GAL4-T155	28	28.1	10	27.8	26	28.3
GAL4-GR1	15	28.9	19	12.4	—	—
GAL4-CY2	27	26.8	19	19.0	27	14.6

The coefficient of variation (CV) is computed from the standard deviation divided by the mean of the data.

CONCLUSIONS

To summarize, we developed a quantitative method for obtaining the relative strength of GAL4 drivers in living tissues. The main technical advantage of this technique is twofold. First, our technique allows comparison of data taken from different times. Second, through the AOTF-dependent tuning our assay enables a straightforward comparison of samples with very different levels of fluorescence. For the chosen set of GAL4/UAS pairs, the GFP-based measurement of the relative protein levels correlated well with the measurement of the relative overall transcript levels and with the biological effects of the drivers. The fluorescence-based quantitation is advantageous since it allows us to focus on a narrower time window within a particular developmental stage and specifically investigate the columnar follicle cells of the egg chamber. The rank of the GAL4 drivers presented here is valid for the first half of stage 10A. Having a calibrated panel of GAL4 drivers enables quantitative analysis of cellular responses in developing tissues. The imaging-based strategy described here can be used to compare a wide range of GAL4/UAS pairs in *Drosophila*, as well as GAL4/UAS systems in other model organisms. Finally, our technique is applicable for quantitation of fluorescent systems in general.

MATERIALS AND METHODS

Fly Stocks

Four GAL4 drivers were used: GAL4-55B, GAL4-T155, GAL4-GR1, and GAL4-CY2. UAS-2EGFP-AH3 was obtained from the Bloomington Stock Center (Bloomington, IN) and described in Halfon *et al.* (2002). UAS-EGFR1-EGFP[1E] and UAS-Kekkon1-EGFP[59] were gifts from J. Duffy. All three UAS constructs encode the enhanced green fluorescent protein (EGFP), a GFPmut1 variant that contains the double-amino-acid substitution of Phe64 to Leu and Ser65 to Thr (Cormack *et al.,* 1996).

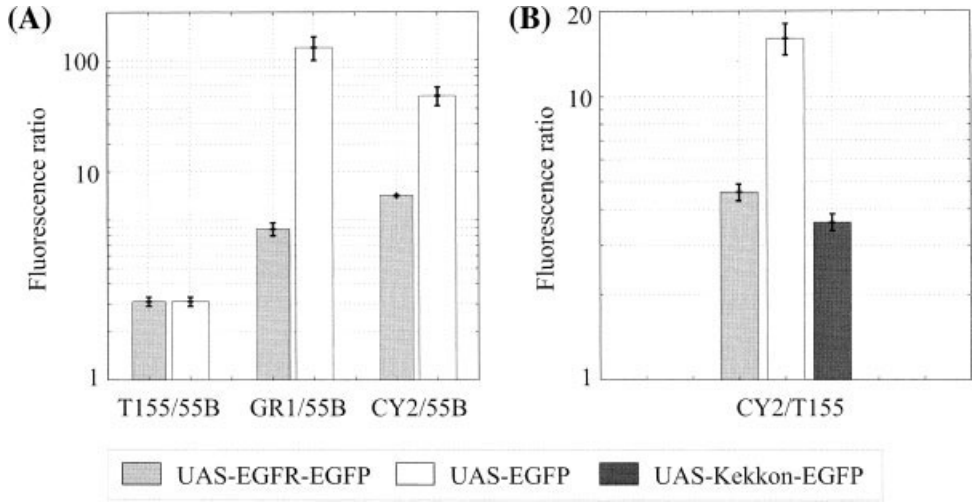

FIG. 4. The relative strength of the GAL4 drivers at early stage 10A of oogenesis (also see Table 2). **a:** The relative strength of the GAL4 drivers measured in UAS-EGFR-EGFP (gray bars) and UAS-EGFP (white bars). **b:** The relative strength of GAL4-CY2 and GAL4-T155 measured in three different UAS lines, including the UAS-Kekkon1-EGFP (dark gray bars). The measured ratios are reproducible with a coefficient of variation of 10%.

Table 2
Measured Fluorescence Ratios in Three UAS Responder Lines

	CY2	GR1	T155	55B
UAS-EGFR-EGFP				
CY2	1	0.6 ± 0.1	0.22 ± 0.02	0.07 ± 0.01
GR1	1.6 ± 0.2	1	0.35 ± 0.03	0.11 ± 0.01
T155	4.6 ± 0.3	2.8 ± 0.3	1	0.32 ± 0.02
55B	14.2 ± 0.1	8.8 ± 0.8	3.1 ± 0.2	1
UAS-EGFP				
CY2	1	2.3 ± 0.1	0.06 ± 0.01	0.019 ± 0.003
GR1	0.41 ± 0.02	1	0.026 ± 0.002	0.008 ± 0.001
T155	16 ± 2	38 ± 3	1	0.31 ± 0.05
55B	60 ± 8	120 ± 20	3.1 ± 0.2	1
UAS-Kekk-EGFP				
CY2	1	N/A	0.27 ± 0.02	N/A
T155	3.6 ± 0.2	N/A	1	N/A

For each GAL4/UAS pair we performed 2–3 independent measurements to give 10–30 data points of mean fluorescence intensity (see Materials and Methods). Each fluorescence data was normalized to AOTF = 1 and corrected for instrument fluctuations. The fluorescence ratio was computed from the means of the normalized fluorescence data. The standard error for the fluorescence ratio was computed using Bootstrap sampling. All pairwise comparisons are significant at a 95% confidence level. Each entry in the table represents the relative strength of the GAL4 line in the column to the GAL4 line in the row.

Fly Egg Chamber/Stage Selection and Slide Preparation

Females were placed on yeast ~24 h before dissection. Ovaries were dissected in cold phosphate-buffered saline (PBS) just before imaging. Early stage 10A egg chambers were selected as those in which the follicle cells had just completed the posterior migration and the centripetal migration was not yet visible (staging based on Spradling, 1993). Egg chambers from stages older than S10A were mostly removed and the remaining eggs were washed in cold oxygenated Grace's medium. Slide preparation was modified from Forrest and Gavis (2005). The dissected egg chambers (mostly S10A and younger) were placed on a Mattex glass-bottom dish #1.5 in cold oxygenated Grace's medium. A small coverslip was placed above the egg chambers and extra liquid was removed carefully with a Kimwipe until the egg chambers were lightly pressed to the bottom of the dish. Egg chambers could stay alive for ~30–40 min under these conditions (as judged by their morphology).

Live Imaging and AOTF Tuning

Live imaging was performed to avoid a loss of signal during fixation. Imaging was performed at room temperature using a Zeiss LSM 510 with a 40x C-Apochromat water immersion objective (NA 1.2). The 488 krypton-argon laser was fixed at 30–70% of its maximal power to obtain ~30–40 μW at 5% AOTF, measured through the ×20 Plan Apochromat objective (see laser calibration below). The laser was passed through HT UV/488/543/633, NFT 590, and NFT 490 dichroic mirror and a bandpass 505-550 filter. The 12-bit images were collected in a 512 × 512 raster size with averaging over four frames. Except for the AOTF setting, all other imaging settings were kept constant (scan speed at 7, pinhole at 93, detector gain at 810, detector offset at −0.08, and amplifier gain at 1). For each specimen the AOTF was set to optimize signal collection while avoiding saturation and the value of AOTF used for capturing each fluorescent image was recorded.

Laser Calibration

Instrument fluctuations were tracked by directly measuring the laser power at different times during the imaging sessions. A laser power meter with photodiode detector head was used to measure the laser intensity going through a 20x Plan-Apochromat objective (NA 0.6). Laser calibration was performed every 1–2 h during an imaging session.

Signal Collection

Signal was collected from the side of the follicular epithelium closest to the objective, from egg chambers with random orientation. Since there was no dorsal–ventral

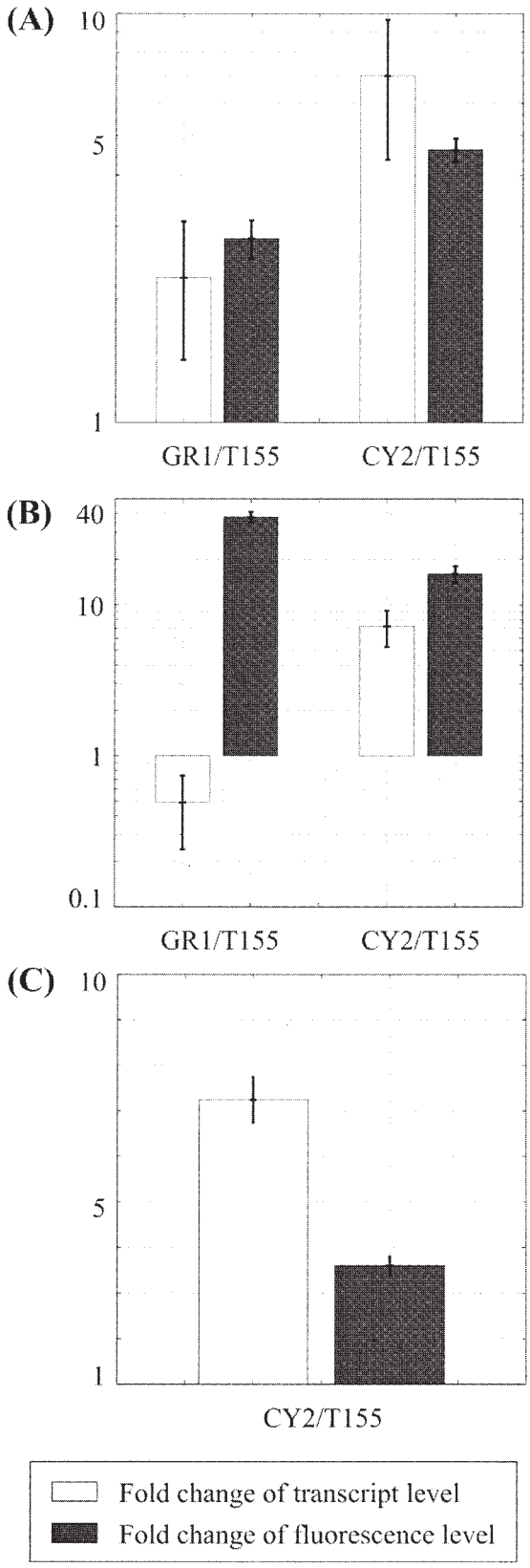

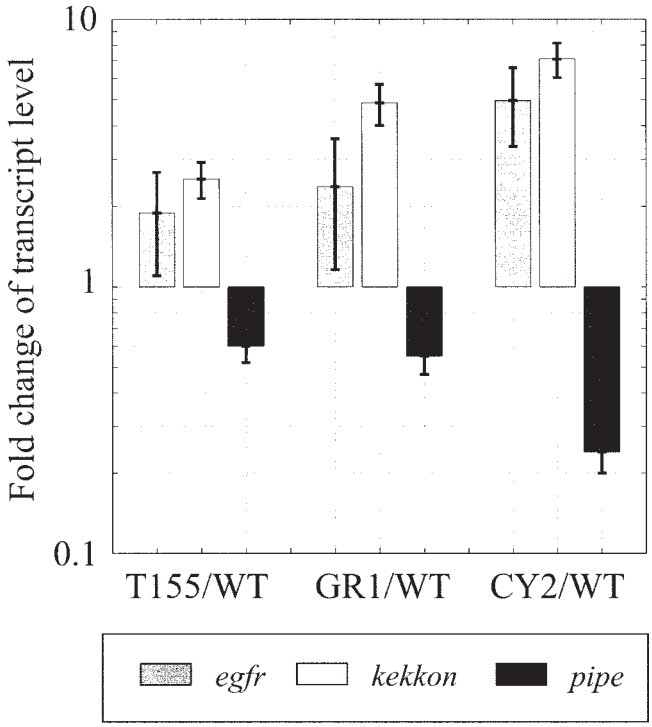

FIG. 6. Transcriptional response of EGFR-target genes to overexpression in EGFR. The qRT-PCR assay was performed in UAS-EGFR-EGFP crossed to three GAL4 drivers (CY2, GR1, and T155). Measurements were performed at stage 9–10 egg chambers. The increase in the level of *egfr* (gray bars) correlates with the increase in *kekkon* (white bars) and the decrease in *pipe* (dark gray bars) expression. All fold changes are statistically significant with $P < 0.05$.

polarity in the expression pattern of the drivers analyzed, a 3D reconstruction in imaging the egg chambers was not necessary. Fluorescent signal was collected from a focal plane that roughly coincided with the apical surface of the follicle cells. For a given UAS construct, the pattern of cellular localization was found to be similar for all the drivers. Thus, the same focal plane within an egg chamber represents roughly the same proportion of the total signal (this is especially true for the uniformly distributed EGFP).

Data Processing

For each image we extracted the fluorescence intensity histogram from the region of interest (ROI) using the Zeiss LSM software 3.2. The ROI was defined as the region within the follicular epithelium where the fluorescence was observed. For T155, GR1, and CY2, the ROI is equivalent to the whole follicular epithelium captured in the image (excluding the out-of-focus outer

FIG. 5. The relative strength of the GAL4 drivers measured with the fluorescence and qRT-PCR assays. White bars correspond to the relative level of *gfp* RNA or transcripts containing a *gfp* sequence; dark gray bars correspond to the relative level of GFP or GFP-tagged proteins. Measurements were performed in UAS-EGFR-EGFP (**A**), UAS-EGFP (**B**), and UAS-Kekkon-EGFP (**C**).

region). For 55B, the ROI was equivalent to an anterior band of 5–10 cell rows. For each fluorescent image of an egg chamber we averaged the fluorescent signal from the entire expression domain and define this quantity as the mean expression level of the corresponding GAL4/UAS pair. The fluorescence data is normalized to AOTF = 1 and to a reference laser power (see the Supplementary Materials for more details).

Statistical Analysis

For each GAL4/UAS pair we obtained a histogram of mean intensities; each histogram was generated from 2–3 independent measurements, with each measurement performed on 6–10 early stage 10A egg chambers (from 2–3 females). The ratio of the protein levels for two given GAL4/UAS pairs was defined as the ratio of the means of fluorescence intensities, obtained from the histogram of fluorescence intensities. The standard error for this quantity was obtained by Bootstrap (Efron and Tibshirani, 1994).

Quantitative Real-Time PCR (qRT-PCR)

All flies were grown at 23°C on standard media and placed on yeast 24 h before dissection. Ovaries were hand-dissected in cold PBS and developmental staging was carried out according to Spradling (1993). Egg chambers from stages 9–10 were separated from older and younger stages and divided into triplicates, such that each sample consists of ~100 egg chambers. Immediately after separation from the ovarioles the egg chambers were put in RNA stabilizing buffer (RNeasy Mini Kit, Qiagen, Valencia, CA). Total RNA was extracted according to the manufacturer's instructions. RNA qualification was performed in a Gene Chip RNA 6000 Nano Assay (Agilent Technologies, Palo Alto, CA). RNA quantification was performed on 1 μl total RNA sample in a NanoDrop ND-1000 spectrophotometer (NanoDrop Technologies, Wilmington, DE). For qRT-PCR, three independent total RNA samples (biological replicates) were prepared for each of the experimental conditions and the wildtype. Each of the samples was analyzed twice, resulting in two technical replicates. Statistical analysis was performed on the groups of three biological replicates with averaging over two technical replicates. One μg of each of the total RNA sample was used for first strand cDNA synthesis using TaqMan Reverse Transcription Kit (Roche, Branchburg, NJ) according to the manufacturer's protocol. For real-time PCR, the reaction consisted of calculated 25 ng first strand cDNA template, primer mix (*egfr*; 5′ end ACCCGATGACTACCTGCAAC, 3′ end GATCCTTGCAGTAGCGGTTC. *kekkon*; 5′ end AGCAGTTTTCCTGGTCCTCA, 3′ end ATGCTCCTCCATTGGCATAC. *gfp*; 5′ end CTGGACGGCGACGTAAAC, 3′ end CGGTGGTGCAGATGAACTT. *pipe*; 5′ end TGTTCATGCACACCAACAAA, 3′ end GATGTGGTTGCCCGTTAGA. *rp49*; 5′ end GACCATCCGCCCAGCATAC, 3′ end ACTGGTGGCGGATGAAGTG), ROX and SYBR Green PCR mix (Stratagene, La Jolla, CA), in a total volume of 25 μl. All expression levels were normalized to the level of *rp49* expression and were calculated using the $2^{(-\Delta\Delta C_t)}$ method (Livak and Schmittgen, 2001). A Student's two-tailed *t*-test was used to determine if the means of the biological replicates from two genetic backgrounds were statistically significant ($P \leq 0.05$). Standard errors were computed by Monte-Carlo sampling from two normal distributions for ΔC_t in control and treatment samples, with means and standard deviations estimated from biological replicates. The qRT-PCR experiments were performed using MX-3000P (Stratagene).

ACKNOWLEDGMENTS

The authors thank Horacio Frydman, Eric Wieschaus, Kevin Foster, Elizabeth Gavis, and Joseph Duffy for help and discussion on the fluorescence assay. SYS, LAG, and NY were supported by funds from the National Science Foundation (NSF), NIGMS (National Institute of General Medical Sciences), Searle Scholar Program, Sloan Foundation, and the Burroughs Wellcome Fund (BWF).

LITERATURE CITED

Alvarado D, Rice AH, Duffy JB. 2004. Bipartite inhibition of *Drosophila* epidermal growth factor receptor by the extracellular and transmembrane domains of Kekkon1. Genetics 107:187–202.

Brand AH, Perrimon N. 1993. Targeted gene expression as a means of altering cell fates and generating dominant phenotypes. Development 118:401–415.

Cormack BP, Valdivia RH, Falkow S. 1996. FACS-optimized mutant of the green fluorescent protein (GFP). Gene 173:33–38.

Dmochowski IJ, Dmochowski JE, Oliveri P, Davidson EH, Fraser SE. 2002. Quantitative imaging of cis-regulatory reporters in living embryos. Proc Natl Acad Sci U S A 99:12895–12900.

Duffy JB. 2001. GAL4 system in *Drosohila*: a fly geneticist's Swiss army knife. genesis 34:1–15.

Efron B, Tibshirani RJ. 1994. An introduction to bootstrap. Boca Raton, FL: CRC Press.

Forrest KM, Gavis ER. 2003. Live imaging of endogenous RNA reveals a diffusion and entrapment mechanism for *nanos* mRNA localization in *Drosophila*. Curr Biol 13:1150–1168.

Ghiglione C, Carraway KL 3rd, Amundadottir LT, Boswell RE, Perrimon N, Duffy JB. 1999. The transmembrane molecule *kekkon 1* acts in a feedback loops to negatively regulate the activity of the *Drosophila* EGF receptor during oogenesis. Cell 96:847–856.

Halfon MS, Gisselbrecht S, Lu J, Estrada B, Keshishian H, Michelson AM. 2002. New fluorescent protein reporters for use with the *Drosophila* Gal4 expression system and for vital detection of balancer chromosomes. genesis 34:135–138.

Hartley KO, Nutt SL, Amaya E. 2002. Targeted gene expression in transgenic *Xenopus* using the binary GAL4-UAS system. Proc Natl Acad Sci U S A 99:1377–1382.

Hirschberg K, Miller CM, Ellenberg J, Presley JF, Siggia ED, Phair RD, Lippincott-Schwartz J. 1998. Kinetic analysis of secretory protein traffic and characterization of Golgi to plasma membrane transport intermediates in living cells. J Cell Biol 143:1485–1503.

Lippincott-Schwartz J, Patterson GH. 2003. Development and use of fluorescent protein markers in living cells. Science 300:87–91.

Livak KJ, Schmittgen TD. 2001. Analysis of relative gene expression data using real-time quantitative PCR and the 2(-Delta Delta C(T)) Method. Methods 25:402–408.

Ornitz DM, Moreadith RW, Leder P. 1991. Binary system for regulating transgene expression in mice: targeting *int-2* gene expression with yeast *GAL4/UAS* control elements. Proc Natl Acad Sci U S A 88: 698–702.

Pawley J. 2000. The 39 steps: a cautionary tale of quantitative 3-D fluorescence microscopy. BioTechniques 28:884–887.

Piston D, Patterson GH, Knobel SM. 1998. Quantitative imaging of the green fluorescent protein (GFP). In: Sullivan K, Kay S, editors. Methods in cell biology: green fluorescence proteins. San Diego: Academic Press. p 31–48.

Piston DW, Patterson H, Knobel SM. 1999. Quantitative imaging of the green fluorescent protein (GFP). Methods Cell Biol 58:31–48.

Queenan AM, Ghabrial A, Schupbach T. 1997. Ectopic activation of *torpedo/Egfr*, a *Drosophila* receptor tyrosine kinase dorsalizes both the eggshell and the embryo. Development 124:3871–3880.

Sandison DR, Williams RM, Wells KS, Strickler J, Webb WW. 1995. Quantitative fluorescence confocal laser scanning microscopy (CLSM). In: Pawley JB, editor. Handbook of biological confocal microscopy. New York: Plenum Press. p 39–53.

Scheer N, Campos-Ortega JA. 1999. Use of the GAL4-UAS technique for targeted gene expression in the zebrafish. Mech Dev 80:153–158.

Sen J, Goltz JS, Stevens L, Stein D. 1998. Spatially restricted expression of *pipe* in the *Drosophila* egg chamber defines embryonic dorsal-ventral polarity. Cell 95:471–481.

Spradling AC. 1993. Developmental genetics of oogenesis. In: Bates M, Martinez AA, editors. The development of *Drosophila melanogaster*. Cold Spring Harbor, NY: Cold Spring Harbor Laboratory Press. p 1–70.